ELSEVIER

Journal of Photochemistry and Photobiology A: Chemistry 139 (2001) 243–251

Journal of Photochemistry and Photobiology A:Chemistry

www.elsevier.nl/locate/jphotochem

Al-doped TiO_2 pigments: influence of doping on the photocatalytic degradation of alkyd resins

Ulrich Gesenhues*

Sachtleben Chemie GmbH, PO Box 170454, 47184 Duisburg, Germany

Received 16 November 2000; accepted 12 December 2000

Abstract

Rutile white pigments are generally doped with Al_2O_3 to suppress their photocatalytic activity, the mechanism of this effect being however obscure. In this investigation, rutile microcrystals were used that had been doped with increasing amounts of Al_2O_3. Parts of the dopant were homogeneously dissolved in the crystal while the rests had segregated to the particle surface. To study the effects of dissolved Al_2O_3 alone, the Al_2O_3 at the surface could be removed by etching. Photocatalytic activities of the pigments with and without surface-Al_2O_3 were determined by artificial weathering of pigmented alkyd paint films and a kinetic analysis in terms of Weibull statistics of failure. Results were interpreted using basic models of photosemiconductors. It is found that the reduction of photocatalytic activities by Al_2O_3 in the bulk is more important than at the surface although its amounts in the bulk are smaller. Bulk-Al_2O_3 dopant states provide efficient recombination sites for the electrical charges photogenerated within the TiO_2 crystal. However, among the two modes of incorporation of Al_2O_3 into rutile only the one providing oxygen vacancies is effective. The slight activity reduction by surface-Al_2O_3 coincides with the reduction of surface hydroxyl concentration measured with these pigments.

Keywords: Semiconductor photocatalysis; Doped titania; Photophysical properties; Photoelectrochemistry; Applied photochemistry; Photodegradation of polymers

1. Introduction

1.1. Photocatalytic activity of TiO_2

Due to its photosemiconductor properties, particulate titanium dioxide may find an application as a photocatalyst, e.g., for the detoxification of waste waters from organic pollutants like textile dyes and herbicides [1,2]. In the established application as a white pigment for paints, plastics, etc. [3], the catalytic activity of titanium dioxide, however, reduces the long-term durability of the polymeric materials and has to be suppressed. Commercial TiO_2 pigments (with the rutile polymorph of TiO_2) are always doped with Al_2O_3 today, yet the way how Al-doping reduces the photoactivity is not known. It is the aim of the present investigation to provide an explanation for this effect.

The basic sequence of reaction steps involved in photocatalysis by TiO_2 is as follows [4,5]. By UV irradiation, e^- in the conduction band and h^+ in the valence band of TiO_2 are generated. Both charge carriers may recombine or be trapped by impurities and dopants within the crystal or at its surface, or they may cross the particle surface and initiate redox reactions of the adsorbed molecules [6–9]. More probably with TiO_2 embedded in paint polymers under ambient conditions, h^+ is transferred to one of the hydroxyl groups always present at the TiO_2 surface [10], and an $^{\bullet}OH$ radical is split off that attacks the polymer. In the presence of O_2 e^- is presumably carried away as an $^{\bullet}OOH$ radical. As this would leave the TiO_2 surface bare of OH groups, initial surface conditions are restored by dissociative adsorption of H_2O [4,5].

It is evident that the photocatalytic activity of TiO_2 depends on various internal and external parameters: dopants, concentrations of surface hydroxyls, electric surface charges accumulated from different rates of consumption of e^- and h^+ outside the particle or from acid–base reactions of the surface hydroxyl groups in aqueous solutions, adsorption of the molecules to be reacted on TiO_2, etc. [11]. In conclusion, although modern research on photocatalysis by TiO_2 is assisted by a variety of novel physicochemical methods [6,12–14,52], mechanistic conclusions may be drawn only from carefully designed experiments.

Investigations of the influence of dopants on the photoactivity of TiO_2 are rare [6,15], and the effects of doping on semiconductor properties and surface hydroxyl

* Tel.: +49-2066222329; fax: +49-2066223329.
E-mail address: ugesenhu@sachtleben.de (U. Gesenhues).

1010-6030/01/$ – see front matter
PII: S1010-6030(00)00429-9

concentrations have not been discriminated. Besides, the effect of surface hydroxyl concentration alone on photoactivity has not been determined reliably up to now [16–18], partly for lack of unambiguous experimental methods to measure surface hydroxyls [10], partly due to the limited knowledge of oxide surface chemistry until recently [19].

1.2. Structures of investigated samples, design of experiments, choice of experimental method

In this work the influence of Al-doping on the photoactivity of TiO_2 is studied using rutile pigments doped with 0–0.8% Al_2O_3, i.e. microcrystals of 0.2 μm size and a specific surface area of 8–9 m^2/g. The distribution of the dopant over the TiO_2 particle as well as the bulk defect structure have been determined for these samples. Accordingly, a part of the dopant is homogeneously dissolved within the rutile crystal while the rest has segregated to the particle surface, the distribution of dopant between bulk and surface being a thermodynamic equilibrium effect with microcrystals [20]. With the highest amount of dopant, the highest bulk concentration is reached, and the rest of dopant forms a complete layer of Al_2O_3 on TiO_2. This layer is, however, still a part of the rutile lattice as follows from measurements of surface acid–base properties [21]. Within the crystal Al^{3+} substitutes Ti^{4+} [22,23] and is charge-compensated by oxygen vacancies [22]. At the largest amount of dopant investigated, Al^{3+} additionally occupies interstitial places [22]

$$Al_2O_3 \rightarrow 2Al'_{Ti} + 3O_O + V_O{}^{**} \quad (1)$$

$$2Al_2O_3 \rightarrow 3Al'_{Ti} + Al_i{}^{***} + 6O_O \quad \text{(Kröger-Uink notation)} \quad (2)$$

For these samples also the concentrations of surface hydroxyls have been measured [24]. Accordingly, the surface of the undoped pigment is fully hydroxylated. By doping the surface hydroxyl concentration decreases steadily to $\frac{3}{4}$ of the saturation value when a complete coverage of the TiO_2 crystal by surface-Al_2O_3 is reached.

So it is the aim of this work to relate the semiconductor bulk properties and surface chemistry of Al-doped TiO_2 to its photocatalytic activity. The influences of electric potentials and adsorption properties on the photocatalytic reactions are excluded in the experiments by using a solid polymer system permeable to O_2 and H_2O wherein the photocatalyst is embedded, i.e. a TiO_2-pigmented paint film. In a standard machine for quality control in the paint and polymer industry, the paint film is artificially weathered and degrades under the continuous influence of light, O_2 and H_2O, i.e. it looses gloss, and a permanent erosion of polymer fragments and liberated pigment particles from the surface begins. From these physical changes the integral degradation rate of the paint film can be extracted by a kinetic model of failure adopted from materials science, the result is a measure of the photoactivity of the pigment [4,5,25,26]. For erosion, the evaluated rate can be corrected for the fraction of the polymer matrix that is not under the influence of TiO_2, and in this way the true value of the pigment's photoactivity is obtained. For the reader not familiar with this application-technological method, explanations are given in Appendix A.

2. Experiments and results

2.1. Materials

Four rutile white pigments were selected from an experimental series where metatitanic acid had been doped with 0–0.8% Al_2O_3/TiO_2 and calcined. Metatitanic acid had been from the sulphate process TiO_2 plant of Sachtleben, Duisburg, hydrous alumina had been used as a dopant, and calcination had followed approved laboratory procedures in manufacturing of TiO_2 white pigments. All calcination products were ball-milled at ca. 3*g* (*g* is the gravitational constant of the earth) as usual, and separated from grit particles by sieving. Details of preparation and properties have been described in [20,22]. Data relevant to the samples investigated here are summarized in Table 1. Besides, total surface hydroxyl concentrations of the pigments have been determined by titration with $LiCH_3$ in diethoxymethane [10,24]; in Fig. 1 the results with these pigments from [24] are plotted in a way to assist the discussion below. For comparison, a pure, fully hydroxylated TiO_2 surface would have 15–23 μmol OH/m^2, and with TiO_2 pigments from the sulphate process, $\frac{1}{8}$–$\frac{1}{4}$ of surface hydroxyls are substituted by $Me_2PO_4{}^-$ and $MePO_4{}^{2-}$ from the calcination additives in metatitanic acid [20,27]. With Al_2O_3-doped pigments, the Al_2O_3 segregated to the particle surface can be removed

Table 1
Properties of investigated TiO_2 pigments

Total Al_2O_3 content (%)	Concentration of Al_2O_3 dissolved in TiO_2 (mol%, rest = TiO_2)[a]	Surface concentration of Al_2O_3 (μmol/m^2)	Specific surface (m^2/g) (before deaggregation)	Calcination temperature (°C)	Rutile content (%, rest = anatase)
0.045	0.038	0.003	8.0	980	99.5
0.214	0.059 ± 0.012	1.85 ± 0.07	8.7	980	99.8
0.478	0.078 ± 0.008	5.15 ± 0.35	8.8	980	100.0
0.793	0.129 ± 0.008	9.00 ± 1.00	8.2	1025	99.9

[a] In all samples 0.038 mol% Al_2O_3 compensate other aliovalent impurities.

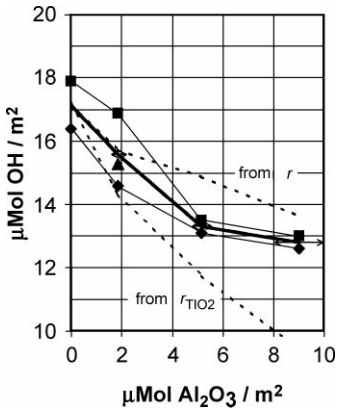

Fig. 1. Measured surface hydroxyl concentrations of Al_2O_3-doped pigments [24] as a function of Al_2O_3 concentrations at the pigment surface from Table 1. Symbols: measured values from double/triple determinations, thick line connects average values, error bars: uncertainty in Al_2O_3 surface concentration. Broken lines: 17.2 × ratio of surface-normalized rates of failure to chalking for a pigment with and without surface-Al_2O_3; in the calculation, integral rates r as well as rates r_{TiO_2} of the polymer exclusively under the influence of TiO_2 have been used.

by etching with aqueous HCl [20], and in this way pigments containing only Al_2O_3 dissolved in the TiO_2 crystal were prepared from the pigments in Table 1. Inevitably, by this procedure the pigments were at the same time deaggregated, and their specific surface area increased by 0.3 (undoped) to 1.1 m^2/g (doped with 0.8% Al_2O_3). Aggregation of primary particles in the pigments is a side-effect of calcination, with the dopant promoting this effect, but the contact area of primary particles is only a small fraction of the total specific surface of the samples given in Table 1.

For comparison, Blanc fixe N, a precipitated barium sulphate from Sachtleben (abbreviated BfN in the following), was used as an inert filler that simulates the influence of TiO_2 pigments on the mechanical properties of a paint but neither absorbs UV light nor is it photoactive. It had a mean particle size of 3.5 μm and a specific surface of 1 m^2/g.

2.2. Experimental methods

Alkyd paints were prepared from the TiO_2 pigments with and without surface-Al_2O_3 and from BfN at a pigment (filler) concentration of 15(14) vol.% (dry), painted onto Al sheets, dried and weathered in a Ci35 Weather-Ometer by Atlas Electric Devices, USA.

The formula of the paint was 61.2% binder, 26.0% pigment or filler, 11.2% solvents, 1.5% driers (Ca-, Co- and Pb-octoates), and 0.1% other additives (application aids). The binder was Uralac AK 419 X-65 from DSM Resins International, Hoek van Holland, the Netherlands, a medium-oil, chain-stopped alkyd resin widely used for car repair, machinery and drum paints. The composition of the solid resin is 48% linoleic rich fatty acids, 26% phthalic anhydride, and 26% pentaerythritol. The paint was prepared by shaking the ingredients for 2 h with glass beads in a Skandex mixer, then it was applied by a doctor blade at a wet layer thickness of 100 μm on Al sheets with a white coil coating priming coat and air-dried for 1 week. Paints with TiO_2 pigments were white and opaque whereas with BfN they were colourless and transparent as seen clearly by applying them to an Al sheet without primer. Because the primer reflected less than 10% of incident UV light, paint films with BfN on primed Al sheets received nearly the same amount of UV irradiation during weathering as the TiO_2-pigmented paint films. Another function of the primer is to assure the same heat absorption of sheets with BfN paints and TiO_2 paints during weathering. In this way weathering experiments with BfN paints will measure the photodegradation of the polymer itself under the same external conditions as with TiO_2 pigmentation.

In the weathering machine samples were continuously irradiated by an IR-filtered Xe arc lamp (spectral distribution of UV and Vis similar to sunlight, i.e. intensities in the UV range decreasing from 400 nm linearly to 0 at 300 nm), and every 18–20th minute samples were rained with demineralized water. Further details are, e.g., described in [28]. As is known from IR spectroscopy and measurements of O_2 uptake and CO and CO_2 evolution, the degradation of polyesters under weathering proceeds via direct photolysis, photo-oxidation and hydrolysis [29,30]. By the first two reaction pathways the UV absorption of the material is reduced continuously [31].

In the experiments colour changes and loss of gloss as well as chalking (=erosion of TiO_2 particles from the paint, only with TiO_2-pigmented paints) were recorded during weathering. Tristimulus-colorimetric parameters R_x (diffuse reflectance of red light), R_y (diffuse reflectance of yellow light) and R_z (diffuse reflectance of blue light) were measured according to ISO 7724 and DIN 5033. Gloss was measured according to DIN 67530 (similar to ASTM D 523-67) at angles of incidence $20 \pm 1^\circ$ and $60 \pm 0.5^\circ$ with unpolarized visible light of spectral distribution of type A (incandescent bulb of 2800 K, DIN 5033). Aperture angles in the plane of incidence were 0.75° (image) and 1.8° or 4.4° (screen), respectively. Gloss values were referred to a plane polished black plate of glass of refractive index 1.567 at 589 nm wavelength. Chalking was determined by the Helmen method explained in Appendix A.

2.3. Results and evaluation

Measured loss of gloss and chalking of TiO_2-pigmented polymer films during weathering are given in Fig. 2. Sixty degree gloss was initially 90–92% and showed the same principal dependence on weathering as 20° gloss. The initial slight decrease of 20° and 60° gloss to an intermediate plateau was due to the evaporation of residual solvent left from drying, final curing processes within the paint and, above all, to the degradation of the uppermost pigment-free paint layer [25] and was neglected in the following. The subsequent development of gloss could be fitted for all measured

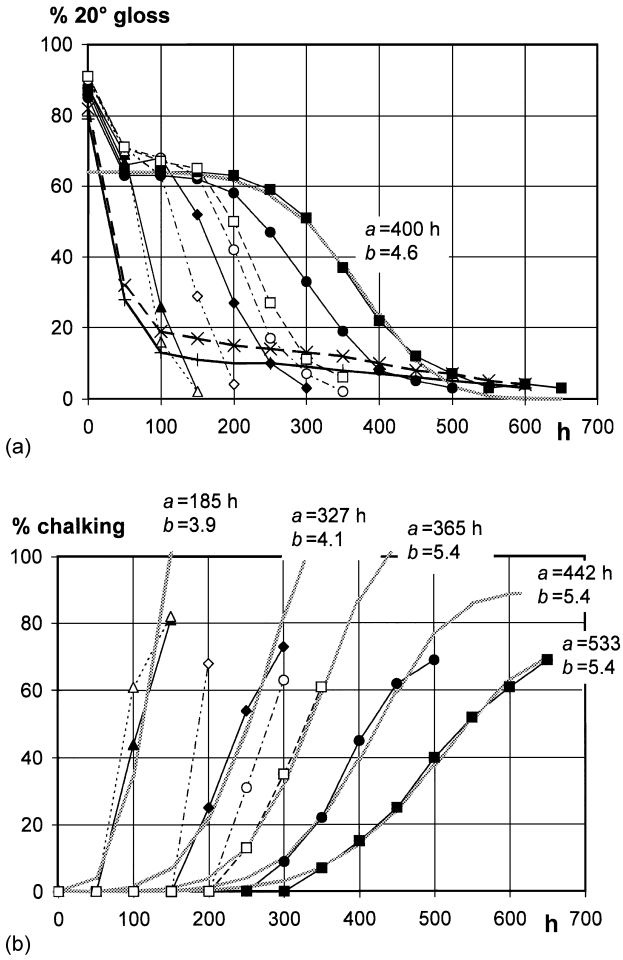

Fig. 2. Loss of 20° gloss (a) and chalking (b) of TiO_2-pigmented and BfN-filled paint films during weathering. TiO_2 pigments doped with 0% (▲, △), 0.2% (◆, ◇), 0.5% (●, ○) and 0.8% Al_2O_3 (■, □); full symbols before, void symbols after HCl etching. Thick grey lines: fit to Eq. (A.1) with results for parameters *a* and *b*. (×) and (+) BfN-filled paint applied directly to the Al sheet and to the primed Al sheet, respectively.

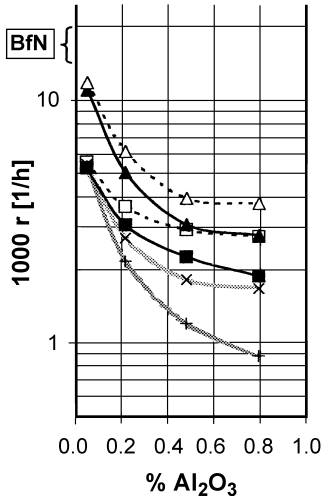

Fig. 3. Rate of paint degradation as a function of the total amount of Al_2O_3 dopant in the TiO_2 pigment. Integral rate *r* of degradation: (▲, △) from loss of 20° gloss and normalized to 9.0 m^2/g specific surface of the pigment; (■, □) from chalking; full symbols before, void symbols after HCl etching. Degradation rate r_{TiO_2} of polymer under the influence of TiO_2, calculated from chalking and normalized to 9.0 m^2/g specific surface of the pigment: (+) and (×) pigments before and after HCl etching. **BfN**: rate of degradation of polymer proper from loss of 20° gloss of BfN-filled paint film.

curves to a first-order statistical process of failure, Eq. (A.1), explained in Appendix A. Also the development of chalking could be fitted satisfactorily to this model although its begin was more abrupt than predicted by Eq. (A.1). Examples demonstrating the goodness of fit are given in Fig. 2a and b. From the fit the integral rates *r* of failure were obtained for the paint films with the various pigments, results are shown in Fig. 3. There, results for loss of gloss have been corrected for the slightly differing specific surfaces of the pigments, as described in Appendix A. Fig. 3 shows that values from loss of 20° gloss are roughly 1.4 times (photostable pigments) to 2.1 times (photoactive pigments) larger than those from chalking. The ratio is characteristic of the polymer system used here, see Appendix A. Integral rates of failure from loss of 60° gloss, although not as reliable, were identical to those from chalking and are therefore omitted in Fig. 3. The fit of Eq. (A.1) to measured curves also yielded values for parameter *b* describing the microscopical spread in the rate of failure. Values of 3.9–5.4 have been determined for chalking, values of 2.9–4.6 for loss of 20° gloss (and values of 2.8–3.8 for loss of 60° gloss). In Fig. 3, for the pigment with 0% Al_2O_3 doping, rates of failure before and after HCl etching nearly coincide, so etching did not create photocatalytically active artifacts at the pigment surface. As changes of brightness and colour during weathering were negligible for all pigments even in the very first periods of weathering where chalking may not yet interfere, it follows that electrons were not accumulated in the TiO_2 particle [4], and any influence of electric potentials on the reaction rate can safely be neglected.

In Fig. 2a also the results for BfN-filled polymer films are shown. For 60° gloss an intermediate plateau was observed from ca. 100–350 h of weathering as for 20° gloss, however at a level of 41–52%. As visual inspection showed, even after 600 h the BfN-filled polymer film had only a few cracks and still completely adhered to the Al sheet (with and without primer). Accordingly, the failure of a BfN-filled film during weathering is a two-step process. First, the smooth surface of the polymer film is eroded layer by layer like TiO_2-pigmented films. At the same time, however, for lack of UV protection of the polymer by BfN, the bulk of the film is transformed photochemically into an embrittled but still coherent layer that has a degradation behaviour of its own. This dominates the second step. In consequence, the rate of failure of the polymer proper to be compared to the rate of failure of the polymer under the influence of TiO_2 must be determined from the *first* step of failure of BfN-filled polymer in Fig. 2a. It is $\frac{1}{50}-\frac{1}{70}$ h^{-1} for 20° gloss. From this value

the rate of failure to continuous erosion is calculated, using the ratio of both rates determined with TiO_2 pigments before, as a direct measurement would not be reliable.

From the integral rates r of failure to erosion, the rates r_{TiO_2} of the polymer domains exclusively under the photocatalytic influence of TiO_2 were calculated for the various pigments, using Eq. (A.2) in Appendix A. Results, with r_{TiO_2} normalized in specific surface, are given in Fig. 3. The ratios r_{TiO_2}/r are 1.0 for the undoped TiO_2-pigment, 0.75 for the pigment with 0.214% Al_2O_3 after etching, then decreasing steadily with decreasing photoactivity of the pigment to a value of 0.45 for the pigment with 0.793% Al_2O_3 before etching. Although this shows that the correction varies with the photoactivity of the pigment and may be quite large, the general shape of pigment photoactivity as a function of the amount of dopant in Fig. 3 is not altered when going from r to r_{TiO_2}.

3. Discussion

Fig. 3 shows that the photoactivity of the pigments first decreases strongly with steadily increasing amounts of Al_2O_3 dopant but then seems to approach a saturation value. In addition, Al_2O_3 at the pigment surface is not as effective as Al_2O_3 dissolved in the crystal, considering the respective amounts of dopant in Table 1. However, the polymer with the undoped TiO_2 pigment still degrades more slowly than the BfN-filled polymer. So, even without doping, the photocatalytic activity of a rutile pigment is not as large as its UV protective effect for this polymer. The ranking of the pigments in photoactivity with respect to Al_2O_3 doping coincides with that found before in the degradation of Ca/Zn-stabilized PVC under identical weathering conditions [32]. However, the spread in pigmentary photoactivity is 2.5 times smaller with the alkyd resin as this polymer is not as stable as PVC whose degradation is *accelerated* by undoped TiO_2 pigments.

These principal conclusions are valid for both parameters recorded here during weathering, i.e. gloss and chalking. For the following extraction of quantitative values of the photosemiconductor properties of the pigments, however, only results from chalking will be used.

3.1. Role of Al_2O_3 dissolved in the crystal

With the pigments investigated here, the concentration of Al_2O_3 dissolved in TiO_2 rises in direct proportion to the total amount of dopant (Table 1), however the products of defect equilibrium 1 reach their maximum concentrations already at a total amount of 0.5% Al_2O_3 [22]. Then the pigmentary photoactivity (both the apparent measure r and true measure r_{TiO_2}) shows nearly the same dependence on the total amount of dopant in Fig. 3 as the concentration of Al^{3+} that is substitutionally incorporated in combination with oxygen vacancies. So it is only this defect structure that seems to suppress TiO_2 photoactivity, and defect structure 2, with interstitially incorporated Al^{3+}, would have no effect.

It is improbable that an Al^{3+} ion in the TiO_2 crystal will act as a deep trap and capture a photogenerated e^- or h^+ as this would correspond chemically to a reduction or oxidation of Al-III. Instead, an oxygen vacancy may trap an e^-, thus restoring the periodicity of electrical charge distribution within the crystal, and subsequently act as a recombination centre for h^+. This concept can be tested by simply taking the rates of failure for the pigments without surface-Al_2O_3 from Fig. 3 and plotting the reciprocal values (=time constants) against the concentrations of Al_2O_3 dissolved in TiO_2 from Table 1. Then a straight line should result for the following reason: the polymer rate of failure is in direct relation to the steady-state concentration of mobile charge carriers in the pigment, and with photoconductors under continuous illumination and modest extraction of photogenerated charges, this concentration is in indirect relation to the concentration of traps as long as there are far more traps than charge carriers, i.e. for low illumination intensities [33]. Further it is assumed that the mobility of charge carriers in TiO_2 does not vary with the degree of doping. In Fig. 4 indeed a fair linear relationship is observed. The intercept on the abscissa corresponds to the amount of Al_2O_3 that is incorporated into rutile compensating other impurities, thus not acting as traps [20]. The pigment with the highest concentration of dissolved Al_2O_3 need not follow the linear relationship because the dopant concentration in excess of the second largest value is incorporated mainly via defect structure 2, i.e. without generating more oxygen vacancies.

Such a plain semiconductor model is applicable here because the type of conductivity of rutile does not change with Al_2O_3 doping. At 900–1000°C and approximately 200 mbar oxygen partial pressure, i.e. the conditions of preparation for the samples, pure rutile is an intrinsic to slight p-type

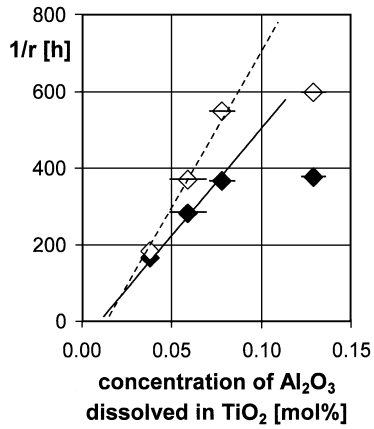

Fig. 4. Test for the action of the Al_2O_3 dopant as a trap for mobile charge carriers in TiO_2 with the results for chalking of polymer films with HCl-etched pigments. Horizontal error bars mark uncertainty in Al_2O_3 concentration from [20]. Full and void symbols: calculated from r and r_{TiO_2}, respectively; ordinate values have been normalized to 9.0 m^2/g specific surface of the pigment.

Table 2
Trapping/recombination efficiencies of bulk- and surface-Al_2O_3 dopant states in rutile pigments, calculated from r (lower value) and r_{TiO_2} (upper value) for chalking, normalized in specific surface

Total Al_2O_3 content of pigment (%)	Bulk Al_2O_3: sphere of influence = cross-section	Surface Al_2O_3: cross-section
0.214	1020–1240	0.48–0.93
0.478	910–1100	0.27–0.60
0.793	510–630	0.22–0.47

semiconductor [34], and rutile homogeneously doped with 0.32% Al_2O_3, i.e. twice the maximum concentration dissolved in the crystals of our samples, is a p-type semiconductor [35].

From the polymer rates of failure for pigments without surface-Al_2O_3, the trapping/recombination efficiency of a bulk-Al_2O_3 dopant state is calculated as $(1 - r_{\text{Al-doped TiO}_2}/r_{\text{undoped TiO}_2})$ divided by the molar fraction of Al_2O_3 dissolved in the crystal. The calculated value may be interpreted as a cross-section when the charges photogenerated in TiO_2 migrate within the crystal, or as a sphere of influence when they diffuse. Although the photogeneration of charges is restricted to approximately the upper 15 nm of a particle, i.e. the penetration depth of UV into TiO_2 [36], trapping and recombination will occur in a thicker layer, due to diffusion. Results of calculations are given in Table 2. They show that the uncertainties in the values for rates of failure have only modest consequences. Accordingly, at low concentrations the Al_2O_3 dopant state is a very efficient trap, and the values for the sphere of influence do agree by magnitude with the efficiency of an oxygen vacancy in Al_2O_3-doped rutile to extinguish IR lattice vibrations [22]! As both effects are based on the range of Coulomb forces within the crystal, this coincidence of results lends support to the model of an oxygen vacancy acting as a trap/recombination centre.

The energy level of the Al_2O_3 dopant state $(2Al'_{Ti} + V_O{}^{**})$ between valence and conduction band of rutile has not been determined up to now, however the following estimate can be made. Let us assume the *hypothetical* defect equilibrium

$$2TiO_2 \rightarrow 2Ti_{Ti} + 3O_O + V_O + \tfrac{1}{2}O_2 \quad (3)$$

for partially reduced rutile TiO_{2-x}, i.e. with Ti^{4+} instead of Ti^{3+} ions and an oxygen vacancy with two localized e^-. Then the dopant state at infinite dissolution, $(2Ti_{Ti} + V_O)$, would be a donor with ionization energies that correspond to those of a He atom in a homogeneous medium having the dielectric function of rutile. Energy levels approximately 0.6 and 1.2 eV below the conduction band edge have been calculated for this model [37]. Now, the Al_2O_3 dopant state $(2Al'_{Ti} + V_O{}^{**})$ is an acceptor whose energy levels, to a first approximation, must be symmetric to those of the hypothetical TiO_{2-x} dopant state $(2Ti_{Ti} + V_O)$ with respect to the mid of the bandgap, following the simple rules for the hole formalism in semiconductors.

To suppress the photoactivity of TiO_2, oxygen vacancies may be implanted into the rutile lattice by doping with oxides of a variety of other tri- and bivalent metals. However, these do not allow the production of white pigments, by imparting colour to the crystal (Fe, Cr) or inhibiting crystal growth and complete transformation to rutile (Mg).

3.2. Role of Al_2O_3 at the particle surface and role of surface hydroxyls

A comparison of polymer rates of failure for pigments with and without surface-Al_2O_3 in Fig. 3 shows that the dopant at the particle surface may reduce the photocatalytic activity slightly, at maximum by a factor of 1.3–1.9 for a monolayer of Al_2O_3. For failure to chalking, the photoactivity reductions reached by increasing coverages of the TiO_2 pigment with Al_2O_3 have been calculated by dividing to the rates of failure for each pigment after and before etching and are plotted in Fig. 1. From the same data, also cross-sections have been calculated for the efficiency of surface-Al_2O_3 dopant states as trap/recombination centres. Results are given in Table 2. These values are much smaller than those for bulk-Al_2O_3, and with very low Al_2O_3 concentrations a value of 1 may be approximated at best. This is astonishing because surface states are known historically as efficient traps/recombination sites that may even disturb the function of semiconductor electronic devices, and internal monolayers and submonolayers of dopants in GaAs have been shown to be effective barriers for mobile charge carriers [38]. For the findings with Al_2O_3-doped pigments, in the following three different explanations are offered that are open to future experimental verification:

1. Within the bulk of partially reduced TiO_{2-x} and at its surface e^- can be stored in empty d orbitals of Ti [39,40] where it may recombine with h^+ later, or it may be promoted into the conduction band by NIR and Vis irradiation [4]. So, if the surface of Al_2O_3-doped TiO_2 has the defect structure of Eq. (2), at low surface concentrations of the dopant e^- may be trapped by Ti ions at the surface, and with high surface concentrations eventually by Ti ions just below.
2. At the surface of partially reduced TiO_{2-x} oxygen vacancies and Ti^{3+} ions have been identified under UHV conditions [2,39–45], proving defect structure Eq. (4) for the surface of undoped TiO_2:

$$2TiO_2 \rightarrow 2Ti'_{Ti} + 3O_O + V_O{}^{**} + \tfrac{1}{2}O_2 \quad (4)$$

So, if the surface of Al_2O_3-doped TiO_2 has the analogous defect structure Eq. (1), the oxygen vacancy will act as a trap for e^-. However, it will not be an efficient trap at the surface: a trapped electron cannot be stabilized as easily as in the bulk because the surrounding lattice is only semi-infinite, reducing the Madelung potential at this site [46] and the redistribution of electron charge density into the direction of neighbour cations [40,47].

3. Both models discussed before do not consider the hydroxylation of the TiO_2 surface although this aspect is important in photocatalytic reactions at the TiO_2 surface. In Fig. 1, the reduction in photocatalytic activity of TiO_2 by surface-Al_2O_3 is compared to the decrease of surface hydroxyl concentrations by Al_2O_3 doping. Considering the uncertainties of measurement and evaluation, coincidence is observed to a large extent. So the photochemical reactions at the pigment surface may follow the simple rate law

$$\nu \sim [^{\bullet}OH] \sim [h^+][I\text{–}OH] \quad (5)$$

where ν is the overall rate of photocatalytical reaction per unit surface of photocatalyst, $[^{\bullet}OH]$ the surface concentration of OH radicals; $[h^+]$ is the surface concentration of defect electrons, being fixed by the processes of photogeneration, trapping and recombination of charges within the crystal; [I–OH] is the surface concentration of hydroxyl groups. However, it is the *total* concentration of surface hydroxyls that has been measured for the Al-doped pigments, and according to Gesenhues [27], only the *acidic* OH at the surface of a TiO_2 crystal should be photocatalytically active. This argument will need a more careful consideration, including the acid–base properties of the pigments, in a forthcoming paper [21].

Acknowledgements

The author thanks R. Optehostert and I. Reinhard for the experimental work as well as Dr. T. Rentschler for the determination of surface hydroxyl concentrations.

Appendix A

A.1. Weathering of TiO_2-pigmented polymer films

Paint films, like other polymer-made fabrics, degrade under the influence of sunlight (UV and heating), O_2 from the air and H_2O as moisture or rain. The degradation shows up first in minute chemical changes [29] often accompanied by colour changes. Then a steady loss of mass of the polymer sets in that proceeds layer by layer from the original surface to the interior. Simultaneously gloss is lost rather abruptly, and with TiO_2-pigmented paints so-called chalking begins [5,25,26,48,53]. The last three physical effects are the ultimate and irreversible consequences of polymer chain scission reactions during degradation: the degraded polymer material is washed away from the surface of the paint film by raining during weathering. The TiO_2 pigment homogeneously dispersed over the polymer is laid free in this way, although still adhering weakly to the polymer. However, it can be wiped off like chalk from the blackboard (→ name of the effect) or collected by an adhesive tape (quantitative determination of chalking by the Helmen method [49]). The method, relying on nephelometry, is an advantage with respect to precision and labour over chemical analysis of degraded paint material or gravimetric recording of the mass loss of a paint film. Anyway, the rates of mass loss and chalking during weathering are in direct relation. It is the general experience with paint films that the 20° gloss, being very sensitive to surface defects, reduces inevitably from 80 to 90% at the begin of weathering to a few percent whereas the terminal value of the 60° gloss may vary between 0 and approximately 35%, depending on paint formula and level of pigmentation. The steady-state rates of mass loss and chalking attained after the initial period of weathering are functions of polymer stability and pigment photoactivity. Of course, the rate of chalking additionally depends on the level of pigmentation of the paint.

As the degradation of polymers generally runs via several parallel and consecutive reactions, it may be advantageous to follow the integral turnover of the photocatalytic reaction by the macroscopic physical changes described above rather than trace the turnover of individual intermediates or products by spectrometry. Besides, the absorption signals of these species in the UV, Vis and IR range are obscured by the strong absorptive or scattering properties of the pigment. As a partially reduced TiO_2 crystal has a strong characteristic broad absorption in the Vis range, Vis spectroscopy can however be used to check whether in the initial period of photocatalytic polymer degradation electrons are consumed as fast as holes [4].

Chemical changes during polymer degradation are recognized after some hours to days of weathering and accumulate to mechanical defects during days and weeks, however the photogeneration and recombination of charges within TiO_2 as well as their transport to/across the semiconductor surface occur within ns to ms as known from semiconductor-physical and electrochemical experiments [1,2,6,14,29,34,35,50,52]. Thus the reactions within the polymer are the rate-determining steps in the photocatalytical degradation of pigmented paint films, and the charge carrier concentrations in the semiconductor-bound steps before will keep steady-state values throughout the weathering experiment. These concentrations will depend on the intrinsic photostability of the specific polymer [25,49] (constant in our experiments) and the photocatalytic quantum efficiency of the TiO_2 particles (varying with the degree of doping). As the efficiency is always far below 100% [1,15] and as the UV extinction cross-section of a rutile white pigment particle is approximately at least three times its geometrical

cross-section [51], TiO_2 pigments in a material also have a UV shielding effect. It follows from these considerations that the same TiO_2 pigment may appear as a UV stabilizer in one polymer and a photocatalyst in the other [4].

A.2. Kinetic model of physical polymer degradation

From several decades of application-technological experience with TiO_2-pigmented paint films, also the physical changes during the initial period of weathering are well understood today [5,25,26,48]. Due to chemical degradation of the polymer, mechanical stress in the paint film increases linearly with time. When the mechanical strength of the film is surpassed, cracks evolve at the surface, degraded polymer is washed away, and loss of gloss as well as chalking set in. As mechanical strength shows a microscopic distribution over the polymer sample, loss of gloss as well as the development of chalking till steady state follow the statistics of failure. An appropriate mathematical model of this process is the cumulative Weibull distribution [48]

$$F(t) = 1 - \exp\left[-\left(\frac{t}{a}\right)^b\right] \tag{A.1}$$

where F is the fraction of microscopic sites having failed after duration t of load, a the time constant of a microscopic first-order process of failure, and b the spread of strength among microscopic sites. If a macroscopic parameter is to be fitted to Eq. (A.1), the difference of values measured at the beginning and at steady state of weathering will correspond to the total sum of defect sites in Eq. (A.1). As gloss and chalking are easily measured with paint films during weathering, the rate of failure, $r = 1/a$, can be determined as a function of the photocatalytic activity of the pigment in the paint from the development of these parameters in the initial period of weathering. This saves a lot of time since extended measurements in the steady-state domain of weathering are no longer necessary. However, values of r determined from loss of gloss and from chalking may diverge, depending on the polymer system [49]. This is because chalking measures simply the sum of pigment loss at all microscopic domains on the polymer film surface. In contrast, gloss is a macroscopic morphological nonlinear quantity that responds to the actual geometrical contour of the film surface as well as to the optical properties of the material in a layer of some 100 nm thickness below the surface [28]. Therefore values of r from chalking will be preferred for the quantitative determination of pigment photoactivity.

The integral rate r_m of mass loss of the pigmented polymer film during weathering may be split into the contributions from the polymer that is under the influence of TiO_2, and from the pigment-free polymer domains:

$$r_m = X r_{TiO_2} + (1 - X) r_{polymer} \tag{A.2}$$

where X is the volume fraction of the polymer under the influence of TiO_2, r_{TiO_2} the rate of degradation of this fraction, and $r_{polymer}$ the rate of degradation of polymer proper. As not r_m, but r_{TiO_2} is the correct quantitative measure of the photoactivity of a pigment, X should be as large as possible to minimize errors. Because mass loss and chalking are directly related, their rates of failure are identical, and the integral rate of chalking can be split up in the same way as r_m in Eq. (A.2). Thus Eq. (A.2) may be applied to check the reliability of results for the integral rate of failure as a measure of the photoactivity of the pigments, using results for $r_{polymer}$ and X from separate experiments.

This model has been used before to determine the photoactivities of various TiO_2 pigments in PVC [28,32].

A.3. Standard procedures of measurement and evaluation

In the paint industry, chalking is determined by collecting the loose pigment particles from the surface of the degraded paint film at regular intervals with a transparent adhesive tape and measuring its transparency (DIN 53223 and Helmen chalking-tester H100). As the reading of % chalking per measuring interval during weathering is in direct relation to pigment mass loss only from 0 to ca. $70\% = 20\,\mu g\,pigment/cm^2$ paint area [49], the steady-state value of chalking attained after the initial period of weathering is reliably measured by this method only for very photostable TiO_2 pigments with normal measuring intervals of 50 h and longer. For the other pigments the value can, however, be determined by fitting values measured in the linear calibration range of % chalking, i.e. during the initial period of weathering, to Eq. (A.1) (*evaluation step* 1). Proper solutions must satisfy two conditions: (1) proportionality between the steady-state value of chalking and the rate r of failure to chalking, (2) identical b values for all samples weathered in one series. This procedure is necessary for an accurate determination of the rate of failure to chalking, although the mathematical form of Eq. (A.1) allows for some error in the steady-state value of chalking.

Next, for the same experimental series the rate r of loss of gloss is obtained from a direct fit of measured loss of 20° gloss to Eq. (A.1), and the characteristic ratio of r values from chalking and loss of gloss is calculated for the polymer system under consideration. By measuring loss of gloss of a nonpigmented paint film during weathering, $r_{polymer}$ is determined in the same way and recalculated into the corresponding value for mass loss (step 2), using the ratio of r values evaluated before.

For the polymer fraction X under the influence of the TiO_2 pigment, a minimum value of 45% is calculated from the TiO_2 pigment volume concentration in the paint formula used in this work and the pigment's UV extinction cross-section [51]. With a photostable TiO_2 pigment this polymer fraction will be fully shielded from UV irradiation. Actually, however, approximately $86 \pm 7\%$ will be shielded with the paint formula used here as with the most photostable commercially available TiO_2 white pigments integral rates of failure between 0.7×10^{-3} and $1.2 \times 10^{-3}\,h^{-1}$ have

been measured for chalking under the same test conditions at the application-technological laboratories of the author's company. An explanation for the larger effective values of X is given in [28]. Now all parameters are available to calculate r_{TiO_2} from r by Eq. (A.2) (*step 3*).

Finally, r values from loss of gloss or chalking are corrected for variations in the specific surface area of the TiO_2 pigments, assuming a proportional relationship (*step 4*). This is because the penetration depth of UV into crystalline TiO_2 is only approximately 15 nm [36], i.e. much smaller than the particle diameter, and the polymer degradation rate will increase with the specific surface of the pigment as any reaction rate in heterogeneous photocatalysis.

References

[1] D.W. Bahnemann, Isr. J. Chem. 33 (1993) 115.
[2] A.L. Linsebigler, G. Lu, J.T. Yates Jr., Chem. Rev. 95 (1995) 735.
[3] H. Heine, et al., Pigments, inorganic, Ullmann's Encyclopedia of Industrial Chemistry, 5th edition, Vol. A20, VCH Publishers, Weinheim, 1992, p. 243.
[4] U. Gesenhues, Double Liaison 43 (1996), Nos. 479–480, 32 (French version including references) and X (English version).
[5] H.G. Völz, G. Kaempf, H.G. Fitzky, A. Klaeren, Photodegradation and photostabilization of coatings, ACS Symposium Series No. 151, 1981, p. 163.
[6] K. Wilke, H.D. Breuer, J. Photochem. Photobiol. A 121 (1999) 49.
[7] J.C.S. Wong, A. Linsebigler, G. Lu, J. Fan, J.T. Yates Jr., J. Phys. Chem. 99 (1995) 335.
[8] G. Lu, A. Linsebigler, J.T. Yates Jr., J. Phys. Chem. 99 (1995) 7626.
[9] J. Fan, J.T. Yates Jr., J. Am. Chem. Soc. 118 (1996) 4686.
[10] T. Rentschler, Eur. Coat. J. 10 (1997) 939.
[11] C.S. Turchi, D.F. Ollis, J. Catal. 122 (1990) 178.
[12] M. Edge, R. Janes, J. Robinson, N. Allen, F. Thompson, J. Warman, J. Photochem. Photobiol. A 113 (1998) 171.
[13] J.M. Kesselman, A. Kumar, N.S. Lewis, in: D.F. Ollis, H. Al-Ekabi (Eds.), Photocatalytic Purification and Treatment of Water and Air, Elsevier, Amsterdam, 1993, p. 19.
[14] H. Gräfe, W. Plieth, Materials Science Forum, Vols. 185–188, Trans. Tech. Publ., Switzerland, 1995, p. 425.
[15] W. Choi, A. Termin, M.R. Hoffmann, Angew. Chem. 106 (1994) 1148.
[16] A.H. Boonstra, C.A.H.A. Mutsaers, J. Phys. Chem. 79 (1975) 1694.
[17] K. Kobayakawa, Y. Nakazawa, M. Ikeda, Y. Sato, A. Fujishima, Ber. Bunsenges. Phys. Chem. 94 (1990) 1439.
[18] Y. Oosawa, M. Grätzel, J. Chem. Soc., Faraday Trans. I 84 (1988) 197.
[19] H.-J. Freund, Ber. Bunsenges. Phys. Chem. 99 (1995) 1261.
[20] U. Gesenhues, Solid State Ionics 101–103 (1997) 1171.
[21] U. Gesenhues, Poster P35 presented at Bunsentagung, Bremen, May 25–27, 1995, Colloids and Surfaces A, Elsevier, Amsterdam, in preparation.
[22] U. Gesenhues, T. Rentschler, J. Solid State Chem. 143 (1999) 210.
[23] J.F. Stebbins, I. Farnan, U. Klabunde, J. Am. Ceram. Soc. 72 (1989) 2198.
[24] T. Rentschler, Farbe & Lack 106 (2000) 62.
[25] K. Rehacek, M. Bradac, Farbe & Lack 102 (1996) 40.
[26] G. Kaempf, W. Papenroth, R. Holm, J. Paint Technol. 46 (1974) 56.
[27] U. Gesenhues, Farbe & Lack 101 (1995) 7.
[28] U. Gesenhues, Polym. Deg. Stab. 68 (2000) 185.
[29] S. Storp, M. Bock, Farbe & Lack 91 (1985) 914.
[30] A.P. Mast, P. Gijsman, FATIPEC Congress Interlaken 1998, Congress Books, Vol. B, p. 279.
[31] L. Cutrone, D.V. Moulton, L.A. Simpson, Pigm. Resin Technol. 17 (1988) 8.
[32] U. Gesenhues, J. Hocken, J. Vinyl Addit. Technol. 6 (2000) 80.
[33] C. Kittel, Einführung in die Festkörperphysik, 3rd Edition, Oldenbourg, Munich, 1973, p. 729.
[34] J. Nowotny, M. Radecka, M. Rekas, J. Phys. Chem. Solids 58 (1997) 927.
[35] J. Yahia, Phys. Rev. 130 (1963) 1711.
[36] U. Gesenhues, Farbe & Lack 100 (1994) 244.
[37] D.C. Cronemeyer, Phys. Rev. 113 (1959) 1222.
[38] M. Heiblum, L.F. Eastman, Spektrum der Wissenschaft, April 1987, p. 86.
[39] V.E. Henrich, P.A. Cox, The Surface Science of Metal Oxides, Cambridge University Press, Cambridge, 1994, p. 187.
[40] U. Diebold, J.F. Anderson, K.-O. Ng, D. Vanderbilt, Phys. Rev. Lett. 77 (1996) 1322.
[41] R.L. Kurtz, R. Stockbauer, T.E. Madey, E. Roman, J.L. de Segovia, Surf. Sci. 218 (1989) 178.
[42] S. Fischer, A. Munz, K.-D. Schierbaum, W. Göpel, Surf. Sci. 337 (1995) 17.
[43] M. Wagner, D.A. Bonnell, M. Rühle, Appl. Phys. A 66 (1998) 1165.
[44] R.A. Bennett, P. Stone, N.J. Price, M. Bowker, Phys. Rev. Lett. 82 (1999) 3831.
[45] G. Lu, A. Linsebigler, J.T. Yates Jr., J. Phys. Chem. 98 (1994) 11733.
[46] D.M. Duffy, J.P. Hoare, P.W. Tasker, J. Phys. C 17 (1984) L195.
[47] A. De Vita, M.J. Gillan, J.S. Lin, M.C. Payne, I. Stich, L.J. Clarke, Phys. Rev. Lett. 68 (1992) 3319.
[48] P. Schutyser, D.Y. Perera, FATIPEC Congress, Amsterdam, 1992, Congress Books, Vol. III, p. 1.
[49] T. Helmen, Farbe & Lack 87 (1981) 181.
[50] R.J. Dwayne Miller, G.L. McLendon, A.J. Nozik, W. Schmickler, F. Willig, Surface Electron Transfer Processes, VCH Publishers, New York, 1995.
[51] B. Proft, Farbe & Lack 104 (1998) 61 and personal communication.
[52] H. Gräfe, W. Plieth, ACH — Models Chem. 132 (1995) 515.
[53] P. Schutzyser, D.Y. Perera, Double Liaison 43 (1996), Nos. 479–480, 47 (French) and XXIV (English).